Tandem synthesis of tetrahydroquinolines and identification of reaction network by operando NMR

Journal:	*Catalysis Science & Technology*
Manuscript ID	CY-ART-03-2021-000418.R1
Article Type:	Paper
Date Submitted by the Author:	19-Apr-2021
Complete List of Authors:	Chen, Jingwen; Zhejiang University, College of Chemical and Biological Engineering Qi, Long; Ames Laboratory, Iowa State University Zhang, Biying; Iowa State University, Department of Chemistry Chen, Minda; Iowa State University, Department of Chemistry Kobayashi, Takeshi; Ames Laboratory, Iowa State University Bao, Zongbi; Zhejiang University, College of Chemical and Biological Engineering Yang, Qiwei; Zhejiang University, College of Chemical and Biological Engineering Ren, Qilong; Zhejiang University, College of Chemical and Biological Engineering Huang, Wenyu; Iowa State University, Department of Chemistry Zhang, Zhiguo; Zhejiang University, College of Chemical and Biological Engineering

ARTICLE

Tandem synthesis of tetrahydroquinolines and identification of reaction network by *operando* NMR

Jingwen Chen, [a] Long Qi, *[b] Biying Zhang, [c] Minda Chen, [c] Takeshi Kobayashi, [b] Zongbi Bao, [a,d] Qiwei Yang, [a,d] Qilong Ren, [a,d] Wenyu Huang *[c] and Zhiguo Zhang*[a,d]

The study of the reaction mechanism and complex network for heterogeneously catalyzed tandem reactions is challenging but can guide reaction design and optimization. Here, we describe using a bifunctional metal-organic framework supported Pd nanoparticles (Pd/UiO-66(HCl)) for the one-pot tandem synthesis of substituted tetrahydroquinolines via Claisen-Schmidt condensation and reductive intramolecular cyclization. The directly observed evolution of intermediates and products, including the reactive species containing hydroxylamine group and an unstable intermediate 2-phenyl-3,4-dihydroquinoline, was enabled by *operando* magic angle spinning nuclear magnetic resonance studies under 50 bar H_2. The reaction network of the heterogeneously catalyzed tandem reaction is deduced based on reaction kinetic information resulted from the *operando* study. The optimized procedure has been applied to various acetophenone and nitrobenzaldehyde derivatives carrying different functional groups, and various valuable substituted tetrahydroquinolines were obtained in moderate to good yields. This work provides a molecular-level understanding of the catalytic system and brings up new opportunities for efficient and sustainable synthesis of medicinally relevant building blocks.

Introduction

1,2,3,4-Tetrahydroquinolines (THQs) architectures widely exist in bioactive natural products[1] and artificial molecules like fragrance, dyes, pharmaceuticals, and hydrogen-storage materials.[2-7] The 2-substituted-THQs,[8] especially the 2-phenyl analogues (PTHQs), have attracted great interest as medicinal scaffolds for treating diseases like estrogen-responsive cancer and osteoporosis.[9,10] Therefore, numerous protocols have been developed for the preparation of PTHQs.[11] The most commonly employed method for generating PTHQs is the hydrogenation of quinolines with various homogeneous and heterogeneous catalysts (Scheme 1).[12-21] However, harsh reaction conditions are usually required because of the high reaction energy barrier in the hydrogenation of quinolines.[22] Other approaches, like oxidative cyclization of amino alcohols,[23] C_α-H activation, and intramolecular nucleophilic substitution,[24,25] have been developed for the synthesis of PTHQs, but the tedious synthetic procedures for the complex starting materials, multiple reaction steps, and harsh reaction conditions significantly restrict their further applications.
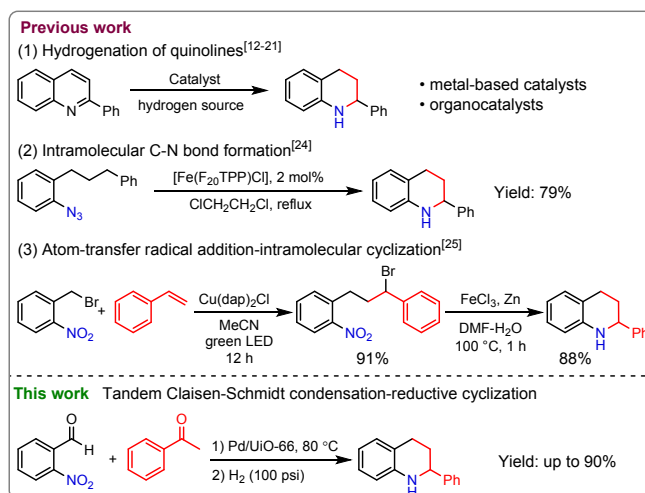
Scheme 1 Representative approaches for the preparation of PTHQ.

Cascade or tandem reactions have attracted tremendous interest continuously because they provide rapid, low cost and simple approaches to preparing complex molecules.[26,27] Many tandem catalysis approaches have been developed for the synthesis of PTHQs.[28-31] Bunce and co-workers[32] reported a reduction-reductive amination reaction of nitro keto esters to prepare 1,2,3,4-tetrahydroquinoline-3-carboxylic esters. Feng's[33] and Kim's group[31] developed the tandem 1,5-hydride transfer/cyclization reaction to afford tetrahydroquinolines. An enantioselective reaction has also been discovered by Han and co-workers,[34] chiral gold phosphate was used to catalyze the tandem hydroamination/transfer hydrogenation of 2-(3-

a. Key Laboratory of Biomass Chemical Engineering of Ministry of Education, College of Chemical and Biological Engineering, Zhejiang University, Hangzhou 310027, China. E-mail: zhiguo.zhang@zju.edu.cn

b. U.S. DOE Ames Laboratory, Iowa State University, Ames, Iowa 50010, USA. E-mail: lqi@iastate.edu

c. Department of Chemistry, Iowa State University, Ames, Iowa 50010, USA. E-mail: whuang@iastate.edu

d. Institute of Zhejiang University-Quzhou, Quzhou 324000, China

† Electronic Supplementary Information (ESI) available. See DOI: 10.1039/x0xx00000x

phenyl-2-propyl)aniline, and PTHQ was obtained in good yield and enantioselectivity. Furthermore, the tandem conjugate addition/cyclization, Michael/Aza-Henry tandem reaction, oxidative cyclization of amino alcohols, etc.[29] have been developed to synthesize tetrahydroquinolines. However, the complicated substrates and tedious separation process of the catalyst and products hinder the practical application of those tandem catalysis approaches. Therefore, the design and development of multifunctional heterogeneous catalysts that can help construct the THQ heterocycles from readily available starting materials in one pot are highly desired. Nevertheless, such tandem catalysis is rather demanding because the formation and cleavage of multiple bonds need to be orchestrated simultaneously and under the same reaction conditions. Additionally, multiple reaction intermediates are typically involved, and byproducts may form during the reaction process, posing challenges in mechanistic investigation and reaction optimization.

Metal-organic frameworks (MOFs) are constructed from metal ions and organic ligands, and multiple functional groups can co-exist and work cooperatively within the porous framework.[35-37] Hence, MOFs have great potential in tandem catalysis,[38-43] and multifunctional MOFs have been reported for obtaining quinoline derivatives by Friedländer reaction or cascade hydrogenation-intramolecular reductive amination.[44-46] Among various MOF reported, UiO-66 (University of Oslo), features 12-coordinated Zr_6 cluster $Zr_6(\mu_3\text{-}O)_4(\mu_3\text{-}OH)_4$, with excellent chemical and thermal stability has been a promising material for catalysis.[47] The coordinatively unsaturated Zr and μ_3-OH work as Lewis and Brønsted acid sites, respectively.[48-50] Corma and coworkers found that UiO-66 and UiO-66-NH$_2$ were efficient in catalyzing the Povarov reaction of an *in-situ* formed imine and dihydropyran, the *trans*-pyrano[3,2-*c*]quinoline was formed in high diastereoselectivity.[51] Besides, our previous work has demonstrated that Pt or Pd nanoparticles-supported UiO-66 can regulate the selective hydrogenation of nitro group in the tandem reaction for the synthesis of bioactive compounds like quinoline *N*-oxides.[52,53] In this work, we synthesized a bifunctional catalyst with UiO-66(HCl)-supported Pd nanoparticles (Pd/UiO-66(HCl)),[54,55] which was anticipated to catalyze the one-pot sequential Claisen-Schmidt condensation and reductive intramolecular cyclization reaction between the 2-nitrobenzaldehydes (NBAs) and acetophenones (ACPs) for the synthesis of PTHQs (scheme 1). The tandem reaction involves multiple intermediates resulting from the simultaneous existence of easily reducible functional groups, which may cause unsatisfactory selectivity toward PTHQs. Understanding the reaction network by monitoring the heterogeneously catalyzed system composed of reactants, intermediates, and favored/disfavored products, is critical in directing the species evolution towards the desired product. The first step of such efforts is to deconvolute individual reaction paths among all existing species and understand their reversibility of interconversions. However, probing a molecular-level reaction pathway is challenging because of the co-existence of solid catalyst, reaction solution, and reactive

gas, particularly when intermediates are not stable during sampling and quantifying processes. Even if intermediates are stable, the limited sampling number results in low-density data points that prevent the accurate delineation of the reaction network.

The *operando* magic-angle spinning nuclear magnetic resonance (MAS-NMR) spectroscopy can operate at high temperatures and pressures,[56] which shown exceptional advantages in acquiring kinetic and structural information of multiphasic reaction systems.[57-59] To elucidate the complex reaction network, we employ *operando* MAS-NMR to detect various stable and unstable reaction intermediates in the tandem reaction for the synthesis of PTHQs. Multiple transient intermediates, including the unstable 2-phenyl-3,4-dihydroquinoline and intermediates with hydroxylamine group, were identified by the *operando* MAS-NMR study under 50 bar H$_2$. The resulted kinetic information of molecules has been utilized to construct the reaction network of the Pd/UiO-66(HCl) catalyzed tandem reaction. The deep insight into the mechanism provides us the opportunity to tune the selectivity for PTHQ. Under the optimized reaction conditions, various functionalized PTHQs were obtained in moderate to good yield by the tandem reaction. This work provides guidance on the rational design of multifunctional heterogeneous catalysts to manufacture complex bioactive molecules efficiently.

Results and discussion

Synthesis and Characterization. UiO-66 was prepared from ZrCl$_4$ and terephthalic acid via a solvothermal reaction with HCl as the modulator in the growth of MOF materials.[60] The resulting sample is denoted as UiO-66(HCl). The powder X-ray diffraction (PXRD) pattern of UiO-66(HCl) was identical to the simulation (Fig. 1A). The Pd nanoparticles (NPs) were introduced to UiO-66(HCl) by an impregnation method.[54] The PXRD pattern of Pd/UiO-66(HCl) indicates that the crystal structure of UiO-66(HCl) was kept after loading Pd precursor and the subsequent reduction process. The Pd amount in Pd/UiO-66(HCl) was 1.6 wt% (Table S2), determined by inductively coupled plasma optical emission spectrometry (ICP-OES). The nitrogen sorption isotherms indicate that both UiO-66(HCl) and Pd/UiO-66(HCl) display a type I isotherm (Fig. 1B) according to IUPAC classification.[61] The Brunauer-Emmett-Teller (BET) surface area of Pd/UiO-66(HCl) is 1687 $m^2 \cdot g^{-1}$ with a micropore volume of 0.55 $cm^3 \cdot g^{-1}$, which are smaller than that of UiO-66(HCl) (BET surface area of 2027 $m^2 \cdot g^{-1}$ and micropore volume of 0.66 $cm^3 \cdot g^{-1}$, Table S1). The results of microscopic study and textual analysis indicated that only a small portion of the internal pore volume of UiO-66(HCl) was occupied by Pd NPs, and Pd/UiO-66(HCl) remains highly porous that allows the free diffusion of reactants and products. Transmission electron microscopy (TEM) images show that Pd NPs are dispersed uniformly on UiO-66(HCl) with a mean size of 3.9 nm (Fig. 2A). The high-resolution TEM (HRTEM) image shows an interplanar spacing of 0.23 nm (Fig. 2B), which corresponds to the (111) lattice spacing of face-centered cubic

(fcc) Pd structure. Besides, another three UiO-66 samples (UiO-66s) has been prepared, including UiO-66 (prepared without acid modulator),[47] UiO-66(AcOH) (prepared with AcOH as the additive),[62] and UiO-66-NH$_2$(0.5) (prepared with mixed linker of terephthalic acid and 2-aminoterephthalic acid; molar ratio 1:1).[60] These three materials are synthesized to investigate the influence of structural modification[63-66] on the catalytic activity, with characterization results shown in Figs. S1-S6.
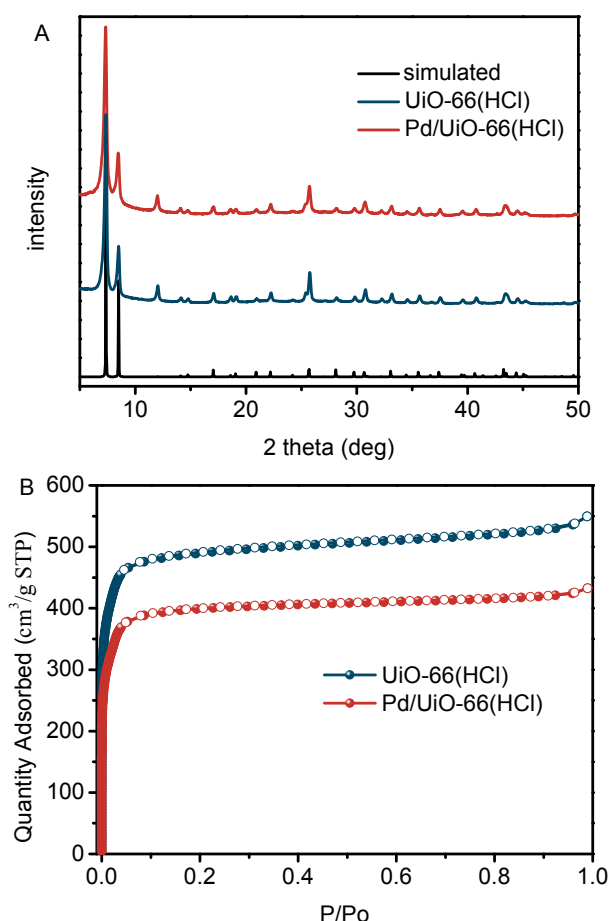

Fig. 1 (A) Powder X-ray diffraction patterns and (B) N$_2$ sorption isotherms of UiO-66(HCl) and Pd/UiO-66(HCl) (1.6 wt%) at -196 °C.
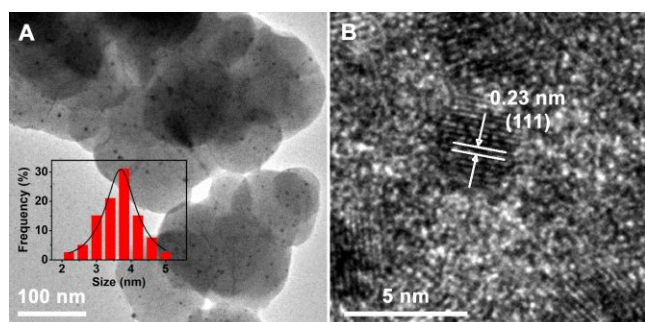
Fig. 2 (A) TEM and (B) HRTEM images of Pd/UiO-66(HCl).

Mechanistic Investigation with *Operando* MAS-NMR. The construction of PTHQ moiety can be achieved via the tandem reaction of readily accessible feedstocks: 2-nitrobenzaldehyde (NBA) and acetophenone (ACP).[53] Several reactive functionalities (–NO$_2$, C=O, C=N, C=C, and arenes) exist in NBA and ACP, and hence a complex reaction network will be present, involving multiple parallel and consecutive pathways and intermediates, products, and byproducts. Traditionally, the exploration of desired reaction selectivity was achieved by laborious trial-and-error experiments. Therefore, it is vital to rapidly identify intermediates and accurately elucidate the complex reaction network promptly for the on-demand control and switch of selectivity. The *operando* high-pressure and high-temperature MAS-NMR spectroscopy enables the detection of both stable and metastable species under reaction conditions. In this context, we employed *operando* MAS-NMR to acquire kinetic and mechanistic information of the multiphasic catalytic production of PTHQ.

Firstly, the Claisen-Schmidt condensation reaction between NBA and ACP was investigated by *operando* MAS-NMR. Our previous work have demonstrated that UiO-66(HCl) possesses large surface area and high catalytic activity for the condensation reaction,[53] hence, the Pd-supported UiO-66(HCl) was chosen as the catalyst for the tandem reaction in the *operando* MAS-NMR studies. To fast-track molecular evolution by ^{13}C NMR, the isotopically labelled ACP with ^{13}C at the acetyl group (195.2 and 24.9 ppm, respectively) was used as the substrate (Fig. 3). Therefore, both intermediates and products derived from ACP can be detected as two doublets of the ^{13}C labels while the unlabeled positions remained invisible in the ^{13}C NMR spectra.
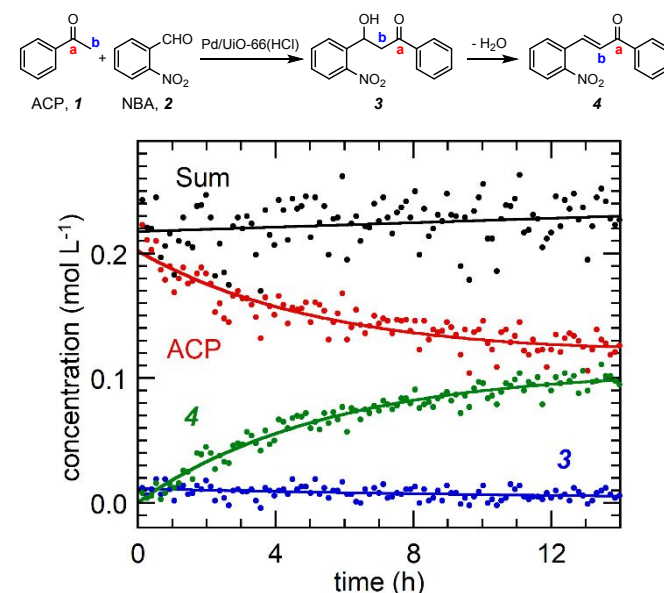

Fig. 3 Kinetic studies of Pd/UiO-66(HCl) catalyzed Claisen-Schmidt condensation of NBA and ACP at 60 °C with *operando* MAS-NMR. Direct polarization ^{13}C MAS-NMR spectra (eight scans per transient) were collected at the MAS rate of 5 kHz. Reaction conditions: ACP-α,β-[13]C$_2$ (1.48 mg, 12.3 μmol), NBA (3.0 mg, 19.8 μmol), toluene (50 μL), 1.6 wt % Pd/UiO-66(HCl) (1.22 mg). The rate of ACP was obtained by fitting the second-order rate equation.

The Claisen-Schmidt condensation reaction was conducted at 60 °C under air. The intensity of ACP resonance decreased immediately upon heating (Fig. 3). At the same time, two new sets of doublets appeared, which can be assigned to β-hydroxyketone intermediate **3** (198.0 and 45.9 ppm) and product 2-nitrochalcone **4** (188.4 and 127.3 ppm), respectively. The β-hydroxyketone intermediate **3** was not observed at higher reaction temperature due to shorter residence time.[53] The concentration profile of ACP, intermediate **3**, and product **4** were extracted from the NMR array, and the overall concentration remains constant over the reaction course. After 14.5 h, the yield of **4** from ACP was 44% with a nearly quantitative selectivity. Furthermore, the reaction kinetics of ACP was curve-fitted with a second-order reaction rate equation, and the pseudo-second-order rate constant of ACP was 0.31 $M^{-1}\cdot h^{-1}$.

To accelerate the conversion of ACP and reduce the possible influence of the unreacted ACP on the next step, the mixture was further heated at a higher reaction temperature (100 °C). After an additional 2.5 h, 74% yield of **4** from ACP was reached, and the selectivity of **4** remained >99% (Fig. S7).

After the Claisen-Schmidt condensation reaction, the high-pressure MAS rotor was further charged with 50 bar H_2; the reaction was carried out at room temperature, monitored by MAS-NMR (Fig. 4). The chalcone **4** reacted rapidly, and its resonances disappeared within 1 h along with multiple new sets of doublets. The emergence of new signals results from the reactions of several reduceable functionalities in **4**, intermediates, products, and byproducts. The signals of PQ (155.9 and 117.5 ppm) only became visible in ~4.5 h, and its concentration kept below 0.02 mol L^{-1} (Fig. S8); hence, PQ is unlikely the intermediate for the formation of PTHQ (55.2 and 30.2 ppm), even though PQ has been suggested as a precursor for the production of PTHQ in several previous reports.[3,11]

Multiple resonances can be identified in the range of 190.5 to 188.4 ppm, attributed to the a-carbon of nitrochalcone **4** and its nitro-reduced intermediates: hydroxylamine **9** and amine **12**. At the same time, the carbonyl and C=C are untouched. The signals of the corresponding b-carbons appear at 121.97 and 121.2 ppm for **9** and **12**, respectively, which has been verified in our recent study.[53] The doublets at 197.5 and 39.43 ppm represent intermediate **7** when C=C is hydrogenated.

The intensities of 164.2 and 22.9 ppm doublets, assigned to 2-phenyl-3,4-dihydroquinoline (**13**), are high throughout the reaction. The detection and quantification of the key intermediate **13** have been a challenge using *ex-situ* analysis due to its air instability. The concentration of **13** increased first and decreased after 4 h, which was proved to be the key intermediate for the formation of PTHQ in the reductive cyclization reaction.[53] Compound **11**, as a necessary compound between **7** and **13**, was not identified in the NMR spectra; it is because of its high reactivity towards cyclization leading to **13**.
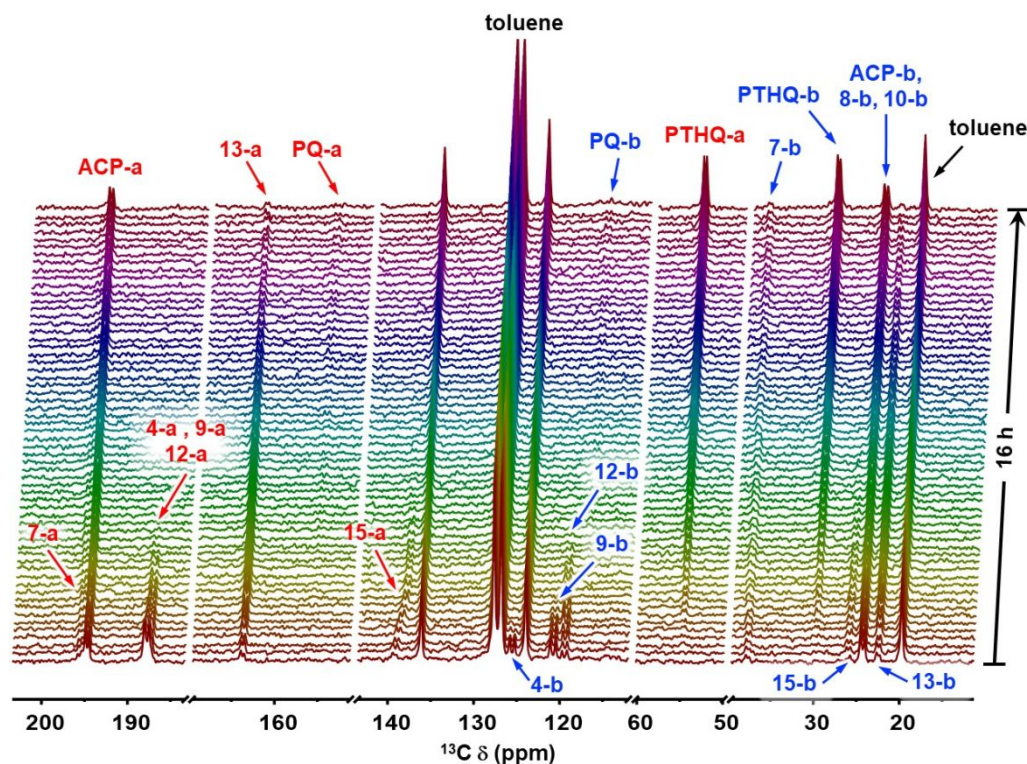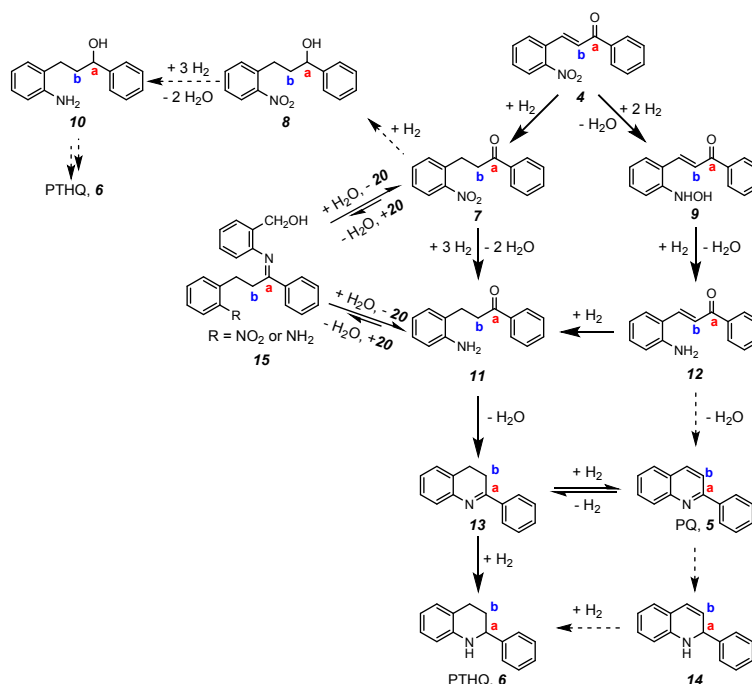

Fig. 4. Time evolution of direct polarization ¹³C MAS-NMR spectra acquired during reductive cyclization of the reaction mixture after the Claisen-Schmidt condensation step (5 kHz MAS rate and eight scans per transient). Reaction conditions: 1.6 wt % Pd/UiO-66(HCl) (1.22 mg), H_2 (50 bar), room temperature, 16 h.

Scheme 2 Reaction network of the Pd/UiO-66(HCl) catalyzed reductive cyclization of 2-nitrochalcone (**4**) in the production of PTHQ based on the *operando* MAS-NMR study. Compound **20** (2-aminobenzylalcohol) is the reduction product of NBA, see **Scheme S1**.

Compound **14** was previously postulated as the intermediate when hydrogenating PQ to PTHQ, which can be isomerized from **13**.[12,67] However, we did not detect **14** because the reduction of PQ or the isomerization of **13** is limited under the reaction condition.

Moreover, a new set of doublets at 139.7 and 26.6 ppm was observed even in the starting spectrum, which has been assigned to the a and b carbons of the imine intermediates (**15**), the condensation product of intermediate **7** or **11** with 2-aminobenzyl alcohol (reduced from NBA, Scheme S1). This compound was only observed in this study when NBA was in excess of ACP. The peak at 139.7 ppm shifted to low frequency gradually, which may be caused by the interaction with byproduct water. Signals of **15** disappeared after 6 h, caused by the hydrolysis to **7** or **11**. The relatively large coupling constant (^{13}C-^{13}C ^1J = 44.6 ppm, Table S3) confirms the double bond functionality. The internal hydrogen bonding of imine N and OH may explain the relatively lower frequency of imine signal.[68,69]

In addition, two new resonance between 66.3 and 72.0 ppm (Fig. S9) were assigned to the carbons in hydroxyl-containing compounds (such as **8** and **10**), which were not observed at lower hydrogen pressure (27.6 bar).

Using *ex-situ* gas chromatography-mass spectrometry (GC-MS), we further confirmed the identities of PTHQ, PQ, **7**, **10**, **12**, etc (Figs. S10-S12). Along with the formation of PTHQ, intermediates **4**, **9**, **12**, and **15** rapidly disappeared. The concentration profiles of quantifiable species in the reductive cyclization are shown in Fig. 5 for those with concentrations higher than PQ, and the production of PTHQ was curve-fitted with pseudo first-order reaction equation (0.25 ± 0.03 h^{-1}).
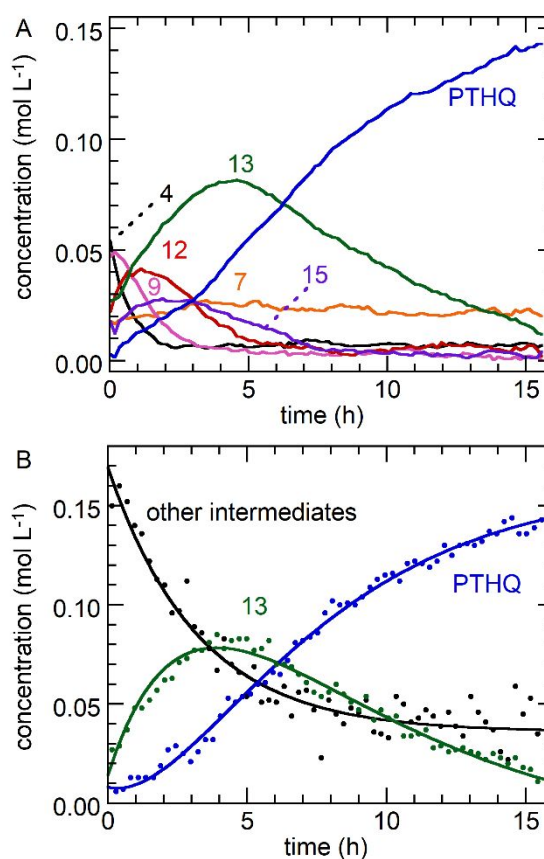

Fig. 5 (A) Time-dependent concentrations of PTHQ, **4**, and other quantifiable intermediates (**7**, **9**, **12**, **13**, and **15**) during reaction derived from MAS-NMR data (**Fig. 4**). Only intermediates with concentrations higher than 0.02 mol L^{-1} are shown. (B) Curvefitting of concentration profiles of PTHQ, key intermediate **13**, and the sum of other quantifiable species (**4**, **7**, **9**, **12**, and **15**).

The above MAS-NMR studies indicated that under 50 bar H_2 atmosphere, the nitro group and C=C bonds could be reduced to generate **7**, **9,** and **12**. The PTHQ product was formed via intermediates **11** and **13** as the major reaction pathway (Scheme 2). Other condensation intermediates and byproducts were formed as well, from the residual ACP or NBA, but are not relevant to the production of PTHQ. Based on the assignment of *operando* MAS-NMR and *ex-situ* GC-MS, the plausible reaction routes of these extra species derived from ACP and NBA are shown in Scheme S1. Both spectroscopic and chromatographic studies indicate the NBA can undergo side reactions, generating side products **20** and **15**, and therefore in the following reaction studies, an excessive amount of ACP was added to ensure full conversion of NBA.

One-pot synthesis of PTHQ. The identification of reaction intermediates by the *operando* MAS-NMR allows us to gain deep understanding of the tandem reaction at molecular level. Accordingly, the reaction conditions were optimized to maximize the PTHQ selectivity.

We first carried out the Claisen-Schmidt condensation reaction with different MOFs as the catalysts at 80 °C. As shown in Fig. 6, UiO-66(HCl) shows high catalytic activity toward the Claisen-Schmidt condensation reaction. UiO-66 prepared without acid modulator shows the lowest activity for the condensation reaction. Compared to HCl, acetic acid as modulator also enhances the rate in a similar fashion. After introducing –NH_2 groups into UiO-66(HCl), the catalytic activity decreased obviously. It should be noted that the TON of UiO-66(HCl) is two orders of magnitude larger than that of UiO-66 (Table S4), which illustrated the vital role of acid modulator in the formation of active sites within UiO-66 framework. Based on the above experimental results, UiO-66(HCl) was employed for further studies.

To optimize the reaction conditions for the hydrogenation step, we first carried out the Claisen-Schmidt condensation reaction at 80 °C for 5 h t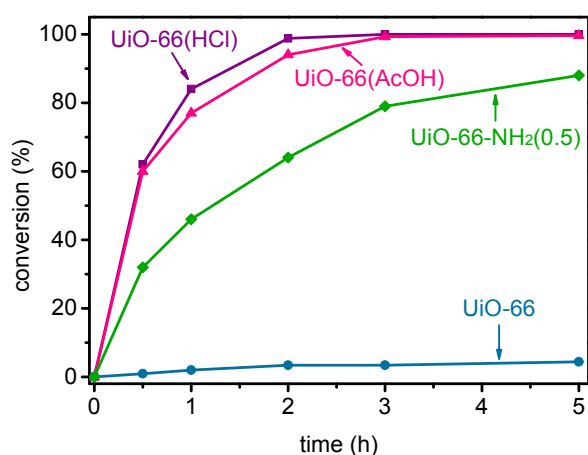o completely convert NBA and ACP to 2-nitrochalcone (**4**) since the reaction selectivity is relatively insensitive to temperature. After that, the reaction mixture was directly charged with H_2 for the reductive cyclization (step 2) without any additional treatment. Lower pressure than 50 bar was attempted to allow sufficient reduction of **13** to PTHQ without over reduction of carbonyls in the reaction mixture.

The catalytic properties of MOF-supported Pd catalysts were evaluated for the hydrogenation reaction of 2-nitrochalcone (Fig S13). High catalytic activity and selectivity of PTHQ were achieved with Pd/UiO-66(HCl) as the catalyst. The activity of Pd/UiO-66(AcOH) is slightly lower, followed by Pd/UiO-66-NH_2(0.5) and Pd/UiO-66. The results demonstrated the beneficial effect UiO-66(HCl) on the supported Pd sites. Besides, the low synthetic temperature for UiO-66(HCl) is attractive for practical application, hence, Pd/UiO-66(HCl) was chosen as the catalyst for further reaction optimization and study of substrate scope.

The influence of reaction temperature on the reductive cyclization step was firstly investigated. As shown in Table 1, PTHQ was obtained in 90% yield in the reductive cyclization of **4** after 8 h (entry 1). The yield of PTHQ decreased to 63% when the reaction temperature was decreased to 40 °C (entry 2). Lowing H_2 pressure from 27.6 bar to 6.9 bar has slight effect on the reductive cyclization reaction, 86% yield of PTHQ was formed after 19 h under 6.9 bar of H_2 (entry 3). It should be noted that PTHQ can be formed smoothly even under ambient-pressure H_2, though with a lower yield (78%, entry 4). Changing the Pd loading from 1.6 wt% to 0.8 wt%, the yield of PTHQ decreased from 86% to 54% (entry 5). Hence, the optimized reaction conditions are (1) 5 h at 80 °C catalyzed by 1.6 wt% Pd/UiO-66(HCl) under air for the Claisen-Schmidt condensation, and then (2) 80 °C under 6.9 bar H_2 for 19 h in the reductive cyclization step. The above-described procedure permits the production of PTHQ from simple and readily available precursors under relatively mild reaction conditions.

Fig. 6 Claisen-Schmidt condensation reaction catalyzed by different MOFs. Reaction conditions: NBA (0.2 mmol), ACP (0.4 mmol), MOF (with 18 mol% of metal), toluene (1 mL), 80 °C.

Table 1 Pd/UiO-66(HCl) catalyzed tandem reaction for the synthesis of PTHQ[a]

entry	H_2 (bar)	time (h)	yield (%)[b]	
			PTHQ	**PQ**
1	27.6	8	90	<1
2[c]	27.6	8	63	7
3	6.9	19	86	2
4	1	19	78	5
5[d]	6.9	19	54	7

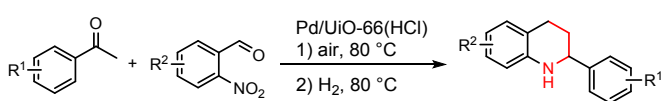[a] Reaction conditions: (1) NBA (0.2 mmol), ACP (0.4 mmol), 1.6 wt% Pd/UiO-66(HCl) (10 mg), toluene (1 mL), 80 °C, 5 h; (2) 80 °C with H_2 of different pressure. [b] Yields were calculated by GC analysis with mesitylene as the internal standard. [c] 40 °C. [d] 0.8 wt% Pd/UiO-66(HCl) as catalysts.
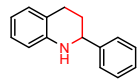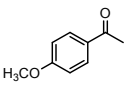
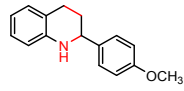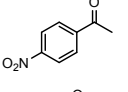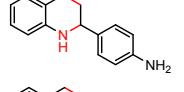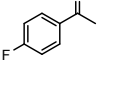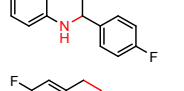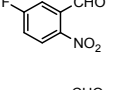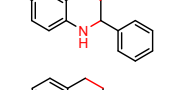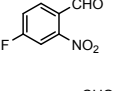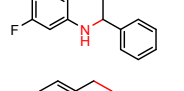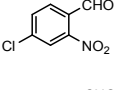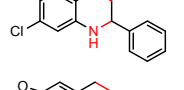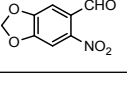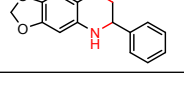No work-up or separation of intermediates is needed, and water is formed as the only innocuous byproduct.

With the optimized reaction conditions in hand, we further explored the substrate scope of Pd/UiO-66(HCl) catalyzed synthesis of PTHQs from NBAs and ACPs bearing different substituents (Table 2). The reaction went smoothly with both electron-donating (R^1 = 4-OCH$_3$, entry 2) and electron-withdrawing (R^1 = 4-NO$_2$, 4-F, entries 3-4) substituents on acetophenone. However, the nitro group was reduced to amine under the standard reaction conditions as expected when 4-nitroacetophenone (entry 3) was used as substrate. Electron-withdrawing substitutes (R^2 = 5-F, 4-F, and 4-Cl, entries 5-7) on NBAs have minor effect on the yield of PTHQs, but the electron-donating group (R^2 = 4,5-(OCH$_2$O), entry 8) reduced the reactivity of NBA and higher H$_2$ pressure and longer reaction time are needed to improve the product yield.

A final set of experiments were conducted to investigate the impact of substrate size on Pd/UiO-66(HCl) catalyzed Claisen-Schmidt condensation. Ketones with different kinetic diameters, acetophenone, 1-acetonaphthone, and 9-acetylanthracene, were employed for this investigation.

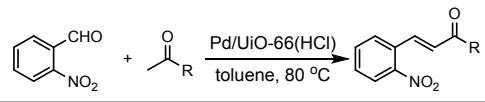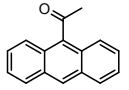**Table 2** Substrate scope of Pd/UiO-66(HCl) catalyzed synthesis of PTHQs.[a]

entry	Ketone	aldehyde	product	yield (%)[b]
1	ACP	NBA		71
2	(4-OCH$_3$ acetophenone)	NBA		60
3	(4-NO$_2$ acetophenone)	NBA		74
4	(4-F acetophenone)	NBA		57
5	ACP	(5-F NBA)		69
6	ACP	(4-F NBA)		89
7	ACP	(4-Cl NBA)		64
8[c]	ACP	(4,5-(OCH$_2$O) NBA)		62

[a] Reaction conditions: (1) NBA (0.2 mmol), ACP (0.4 mmol), 1.6 wt% Pd/UiO-66(HCl) (10 mg), toluene (1 mL), 80 °C, 5 h; (2) 6.9 bar H$_2$, 80 °C, 19 h. [b] Yield of isolated products. [c] 1.6 wt% Pd/UiO-66(HCl) (20 mg); step (1) 80 °C, 10 h and step (2) H$_2$ (27.6 bar), 80 °C, 38 h.

As shown in Table 3, the conversion of NBA reacted with different ACPs was in the following order: acetophenone > 1-acetonaphthone > 9-acetylanthracene, indicating that Pd/UiO-66(HCl) is size-selective in catalysis. The observation of drastically different activities also provides evidence that the Claisen-Schmidt condensation reaction occurs in the pores of Pd/UiO-66(HCl) rather than on the external surface or by leached catalytic species. The effect of size selectivity was also observed in the reductive cyclization reaction catalyzed by Pd/UiO-66(HCl) (Fig. S14).

Table 3. Size-selective Claisen-Schmidt condensation of NBA and different ketones catalyzed by Pd/UiO-66(HCl)[a]

entry	ketone	conversion (%)[b]
1	ACP	85
2	(1-acetonaphthone)	38
3	(9-acetylanthracene)	6

[a] Reaction conditions: NBA (0.2 mmol), ketone (2.0 equiv), 1.6 wt% Pd/UiO-66(HCl) (10 mg), toluene (1 mL), 80 °C, 5 h. [b] Conversion of NBA determined by GC with mesitylene as the internal standard.

Conclusions

In this study, we synthesized a bifunctional catalyst by loading Pd precursor into an acidic MOF followed by reduction to produce Pd nanoparticles supported on MOF (Pd/UiO-66(HCl)). The catalyst showed high performance for the tandem synthesis of PTHQs in one pot. The tandem synthesizing PTHQs in high yield combines Claisen-Schmidt condensation between NBA and ACP, catalyzed by the MOF's acidic sites, and the reduction of *in-situ* produced *ortho*-nitrochalcone, catalyzed by Pd NPs. *Operando* high-pressure MAS-NMR spectroscopy was successfully employed to pinpoint stable and metastable intermediates, in particular, 2-phenyl-3,4-dihydroquinoline and intermediates with hydroxylamine; the explicit quantification of their kinetics allows the elucidation of the reaction pathways. These mechanistic insights, provided by *operando* spectroscopy, clearly demonstrates that a complex tandem chemical transformation could be enabled by catalyst design. This protocol provides a simple and convenient approach for the selective preparation of diverse PTHQs as shown in the substrate-scope study, avoiding tedious separation and purification processes of the reaction intermediates. This reaction mechanism study provides valuable references and guides us to design better multifunctional catalysts to prepare valuable bioactive cyclic compounds.

Conflicts of interest

There are no conflicts to declare.

Acknowledgements

References

1   A. R. Katritzky, S. Rachwal and B. Rachwal, *Tetrahedron*, 1996, **52**, 15031-15070.
2   R. H. Crabtree, *Energy Environ. Sci.*, 2008, **1**, 134-138.
3   V. Sridharan, P. A. Suryavanshi and J. C. Menendez, *Chem. Rev.*, 2011, **111**, 7157-7259.
4   N. Goli, P. S. Mainkar, S. S. Kotapalli, K. Tejaswini, R. Ummanni and S. Chandrasekhar, *Bioorg. Med. Chem. Lett.*, 2017, **27**, 1714-1720.
5   K. Rakstys, J. Solovjova, T. Malinauskas, I. Bruder, R. Send, A. Sackus, R. Sens and V. Getautis, *Dyes Pigments*, 2014, **104**, 211-219.
6   Z. Z. Wei, F. J. Shao and J. G. Wang, *Chinese J. Catal.*, 2019, **40**, 980-1002.
7   P.-Y. Chung, Z.-X. Bian, H.-Y. Pun, D. Chan, A. S.-C. Chan, C.-H. Chui, J. C.-O. Tang and K.-H. Lam, *Future Med. Chem.*, 2015, **7**, 947-967.
8   P. Y. Yao, P. Q. Cong, R. Gong, J. L. Li, G. Y. Li, J. Ren, J. H. Feng, J. P. Lin, P. C. K. Lau, Q. Q. Wu and D. M. Zhu, *ACS Catal.*, 2018, **8**, 1648-1652.
9   O. B. Wallace, K. S. Lauwers, S. A. Jones and J. A. Dodge, *Bioorg. Med. Chem. Lett.*, 2003, **13**, 1907-1910.
10 T. A. Rano, E. Sieber-McMaster, P. D. Pelton, M. Yang, K. T. Demarest and G. H. Kuo, *Bioorg. Med. Chem. Lett.*, 2009, **19**, 2456-2460.
11 I. Muthukrishnan, V. Sridharan and J. C. Menendez, *Chem. Rev.*, 2019, **119**, 5057-5191.
12 G. E. Dobereiner, A. Nova, N. D. Schley, N. Hazari, S. J. Miller, O. Eisenstein and R. H. Crabtree, *J. Am. Chem. Soc.*, 2011, **133**, 7547-7562.
13 M. Yan, T. Jin, Q. Chen, H. E. Ho, T. Fujita, L.-Y. Chen, M. Bao, M.-W. Chen, N. Asao and Y. Yamamoto, *Org. Lett.*, 2013, **15**, 1484-1487.
14 F. Chen, A.-E. Surkus, L. He, M.-M. Pohl, J. Radnik, C. Topf, K. Junge and M. Beller, *J. Am. Chem. Soc.*, 2015, **137**, 11718-11724.
15 M. Rueping, A. P. Antonchick and T. Theissmann, *Angew. Chem., Int. Ed.*, 2006, **45**, 3683-3686.
16 G. Erős, K. Nagy, H. Mehdi, I. Pápai, P. Nagy, P. Király, G. Tárkányi and T. Soós, *Chem.—Eur. J.*, 2012, **18**, 574-585.
17 X. Qiao, Z. Zhang, Z. Bao, B. Su, H. Xing, Q. Yang and Q. Ren, *RSC Adv.*, 2014, **4**, 42566-42568.
18 W. B. Gong, Q. L. Yuan, C. Chen, Y. Lv, Y. Lin, C. H. Liang, G. Z. Wang, H. M. Zhang and H. J. Zhao, *Adv. Mater.*, 2019, **31**, 1906051.
19 L. Tao, Y. Ren, C. Li, H. Li, X. Chen, L. Liu and Q. Yang, *ACS Catal.*, 2020, **10**, 1783-1791.
20 G. Li, H. Yang, H. Zhang, Z. Qi, M. Chen, W. Hu, L. Tian, R. Nie and W. Huang, *ACS Catal.*, 2018, **8**, 8396-8405.
21 X. Yu, R. Nie, H. Zhang, X. Lu, D. Zhou and Q. Xia, *Microporous Mesoporous Mater.*, 2018, **256**, 10-17.
22 T. S. Bush, G. P. A. Yap and W. J. Chain, *Org. Lett.*, 2018, **20**, 5406-5409.
23 K.-i. Fujita, K. Yamamoto and R. Yamaguchi, *Org. Lett.*, 2002, **4**, 2691-2694.
24 Y. Liu, J. Wei and C.-M. Che, *Chem. Commun.*, 2010, **46**, 6926-6928.
25 S. Paria, M. Pirtsch, V. Kais and O. Reiser, *Synthesis*, 2013, **45**, 2689-2698.
26 M. J. Climent, A. Corma, S. Iborra and M. J. Sabater, *ACS Catal.*, 2014, **4**, 870-891.
27 D. Jagadeesan, *App. Cat. A: Gen.*, 2016, **511**, 59-77.
28 J.-C. Hsieh and H.-L. Su, *Synthesis*, 2020, **52**, 819-833.
29 B. Nammalwar and R. A. Bunce, *Molecules*, 2014, **19**, 204-232.
30 H. R. Zhang, Z. W. Dong, Y. J. Yang, P. L. Wang and X. P. Hui, *Org. Lett.*, 2013, **15**, 4750-4753.
31 Y. K. Kang, S. M. Kim and D. Y. Kim, *J. Am. Chem. Soc.*, 2010, **132**, 11847-11849.
32 R. A. Bunce, T. Nago and N. Sonobe, *J. Heterocyclic Chem.*, 2007, **44**, 1059-1064.
33 Z.-X. Jia, Y.-C. Luo and P.-F. Xu, *Org. Lett.*, 2011, **13**, 832-835.
34 Y.-L. Du, Y. Hu, Y.-F. Zhu, X.-F. Tu, Z.-Y. Han and L.-Z. Gong, *J. Org. Chem.*, 2015, **80**, 4754-4759.
35 J. Lee, O. K. Farha, J. Roberts, K. A. Scheidt, S. T. Nguyen and J. T. Hupp, *Chem. Soc. Rev.*, 2009, **38**, 1450-1459.
36 W. Lu, Z. Wei, Z. Y. Gu, T. F. Liu, J. Park, J. Park, J. Tian, M. Zhang, Q. Zhang, T. Gentle III, M. Bosch and H. C. Zhou, *Chem. Soc. Rev.*, 2014, **43**, 5561-5593.
37 S. M. Cohen, *Chem. Rev.*, 2012, **112**, 970-1000.
38 Y.-B. Huang, J. Liang, X.-S. Wang and R. Cao, *Chem. Soc. Rev.*, 2017, **46**, 126-157.
39 Z. Yin, S. Wan, J. Yang, M. Kurmoo and M.-H. Zeng, *Coord. Chem. Rev.*, 2019, **378**, 500-512.
40 A. Dhakshinamoorthy and H. Garcia, *ChemSusChem*, 2014, **7**, 2392-2410.
41 A. Dhakshinamoorthy, A. M. Asiri and H. Garcia, *Dalton T.*, 2020, **49**, 11059-11072.
42 Y. Zhang, C. Huang and L. Mi, *Dalton T.*, 2020, **49**, 14723-14730.
43 M. Hao and Z. Li, *Sol. RRL*, 2020, 2000454.
44 N. Martin and F. G. Cirujano, *Org. Biomol. Chem.*, 2020, **18**, 8058-8073.
45 F. G. Cirujano, A. Leyva-Pérez, A. Corma and F. X. Llabrés i Xamena, *ChemCatChem*, 2013, **5**, 538-549.
46 E. Perez-Mayoral, Z. Musilova, B. Gil, B. Marszalek, M. Polozij, P. Nachtigall and J. Cejka, *Dalton Trans.*, 2012, **41**, 4036-4044.
47 J. H. Cavka, S. Jakobsen, U. Olsbye, N. Guillou, C. Lamberti, S. Bordiga and K. P. Lillerud, *J. Am. Chem. Soc.*, 2008, **130**, 13850-13851.
48 N. L. Drenchev, K. K. Chakarova, O. V. Lagunov, M. Y. Mihaylov, E. Z. Ivanova, I. Strauss and K. I. Hadjiivanov, *JoVE-J. Vis. Exp.*, 2020, e60285.
49 Z. Hu and D. Zhao, *CrystEngComm*, 2017, **19**, 4066-4081.
50 G. Fu, F. G. Cirujano, A. Krajnc, G. Mali, M. Henrion, S. Smolders and D. E. De Vos, *Catal. Sci. Technol.*, 2020, **10**, 4002-4009.
51 V. L. Rechac, F. G. Cirujano, A. Corma and F. X. Llabres i Xamena, *Eur. J. Inorg. Chem.*, 2016, 4512-4516.

52 J. Chen, B. Zhang, L. Qi, Y. Pei, R. Nie, P. Heintz, X. Luan, Z. Bao, Q. Yang, Q. Ren, Z. Zhang and W. Huang, *ACS Appl. Mater. Interfaces*, 2020, **12**, 23002-23009.

53 L. Qi, J. Chen, B. Zhang, R. Nie, Z. Qi, T. Kobayashi, Z. Bao, Q. Yang, Q. Ren, Q. Sun, Z. Zhang and W. Huang, *ACS Catal.*, 2020, **10**, 5707-5714.

54 X. Li, Z. Guo, C. Xiao, T. W. Goh, D. Tesfagaber and W. Huang, *ACS Catal.*, 2014, **4**, 3490-3497.

55 X. Li, T. W. Goh, L. Li, C. Xiao, Z. Guo, X. C. Zeng and W. Huang, *ACS Catal.*, 2016, **6**, 3461-3468.

56 E. Walter, L. Qi, A. Chamas, H. Mehta, J. Sears, S. L Scott and D. Hoyt, *J. Phys. Chem. C*, 2018, **122**, 8209-8215.

57 A. Chamas, L. Qi, H. S. Mehta, J. A. Sears, S. L. Scott, E. D. Walter and D. W. Hoyt, *Magn. Reson. Imaging*, 2019, **56**, 37-44.

58 L. Qi, A. Chamas, Z. R. Jones, E. D. Walter, D. W. Hoyt, N. M. Washton and S. L. Scott, *J. Am. Chem. Soc.*, 2019, **141**, 17370-17381.

59 W. P. Zhang, S. T. Xu, X. W. Han and X. H. Bao, *Chem. Soc. Rev.*, 2012, **41**, 192-210.

60 M. J. Katz, Z. J. Brown, Y. J. Colon, P. W. Siu, K. A. Scheidt, R. Q. Snurr, J. T. Hupp and O. K. Farha, *Chem. Commun.*, 2013, **49**, 9449-9451.

61 K. S. W. Sing, D. H. Everett, R. A. W. Haul, L. Moscou, R. A. Pierotti, J. Rouquerol and T. Siemieniewska, *Pure Appl. Chem.*, 1985, **57**, 603-619.

62 H. Wu, Y. S. Chua, V. Krungleviciute, M. Tyagi, P. Chen, T. Yildirim and W. Zhou, *J. Am. Chem. Soc.*, 2013, **135**, 10525-10532.

63 L. Valenzano, B. Civalleri, S. Chavan, S. Bordiga, M. H. Nilsen, S. Jakobsen, K. P. Lillerud and C. Lamberti, *Chem. Mater.*, 2011, **23**, 1700-1718.

64 G. C. Shearer, S. Chavan, J. Ethiraj, J. G. Vitillo, S. Svelle, U. Olsbye, C. Lamberti, S. Bordiga and K. P. Lillerud, *Chem. Mater.*, 2014, **26**, 4068-4071.

65 M. Vandichel, J. Hajek, F. Vermoortele, M. Waroquier, D. E. De Vos and V. Van Speybroeck, *CrystEngComm*, 2015, **17**, 395-406.

66 W. Liang, C. J. Coghlan, F. Ragon, M. Rubio-Martinez, D. M. D'Alessandro and R. Babarao, *Dalton Trans.*, 2016, **45**, 4496-4500.

67 T. Wang, L.-G. Zhuo, Z. Li, F. Chen, Z. Ding, Y. He, Q.-H. Fan, J. Xiang, Z.-X. Yu and A. S. C. Chan, *J. Am. Chem. Soc.*, 2011, **133**, 9878-9891.

68 K. Neuvonen, F. Fulop, H. Neuvonen, A. Koch, E. Kleinpeter and K. Pihlaja, *J. Org. Chem.*, 2001, **66**, 4132-4140.

69 M. S. Singh and P. Singh, *Synthetic Commun.*, 2008, **38**, 775-783.